IEEE Access
Multidisciplinary | Rapid Review | Open Access Journal

Received March 16, 2021, accepted April 14, 2021, date of publication April 19, 2021, date of current version April 27, 2021.

Digital Object Identifier 10.1109/ACCESS.2021.3073953

Improvement of Noise Stability of Michelson Optical Fiber Voice Monitoring System

YUHAN HU, QIUHENG SONG, HEKUO PENG, AND QIAN XIAO
Department of Material Science, Fudan University, Shanghai 200433, China

Corresponding author: Qian Xiao (ychunww@163.com)

This work was supported in part by the State Key Development Program for Basic Program of China under Grant 2017YFB0803100, and in part by the Project funded by the Science and Technology Commission of Shanghai Municipality under Grant 19511132200.

ABSTRACT Optical fiber sensing is a novel sensing technology with the advantages of anti-electromagnetic interference, anti-corrosion and high sensitivity suiting for many special applications. In this paper, a Michelson optical fiber voice monitoring system is introduced and a novel sound extraction algorithm is proposed to improve the noise stability of it. The voice demodulated by a traditional algorithm based on 3×3 fiber coupler has unstable background noise intensity with the change of the working point of the interferometer. The unstable noise comes from the shot noise of photodetectors. The sound extraction method proposed in this paper uses the relation between shot noise and light intensity to smooth the unstable noise and does not affect the quality of voice monitoring. Voice monitoring systems using this algorithm have stable monitoring quality without any working point control technology. The fluctuation range of noise intensity in 300∼3500 Hz decrease from 10 dB to less than 2 dB compared with the traditional demodulation algorithm. Such a method and system can be widely used in many special voice monitoring application fields such as prison, underground utility tunnel.

INDEX TERMS Optical fiber sensors, shot noise, voice monitoring.

I. INTRODUCTION

Among various sensing technologies, optical fiber sensing is a novel sensing technology rapidly developing in recent years. Compared with traditional electronic sensors, optical fiber sensors have the advantages of anti-electromagnetic interference, anti-corrosion, low cost and high sensitivity [1] suiting for many special applications. The voice monitoring system based on optical fiber sensors [2] is one of the research branches. Voice monitors made of optical fiber sensors have the advantages of small size, anti-interference, good concealment, and can be widely used in many special application fields such as prison, underground utility tunnel, etc.

According to the type of lightwave modulation by sound wave, the type of optical fiber sensors used for voice detection can be divided into intensity modulation, phase modulation, and polarization modulation. Among them, phase modulation optical fiber sensors have high sensitivity without special structural design. Phase modulation optical fiber sensors have a variety of structures, for instance, Sagnac interferometer (SI) [3]–[5], Michelson interferometer (MI) [6], Mach-Zender interferometer [7], Fabry-Perot interferometer [8], Fiber Bragg grating (FBG) [9], phase-sensitive optical time-domain reflectometer (φ-OTDR) [10] and some hybrid structures of them [11], [12]. SI and MI have the advantages of simple structure, low manufacturing cost, and anti-polarization fading. Compared with SI, no delay coil is required in MI, which makes systems based on MI smaller and more suitable for practical applications.

In this paper, we study the optical fiber voice sensor based on MI and the corresponding sound extraction algorithm. Our research found that MI-based optical fiber voice sensor has the problem of unstable background noise. The power of background noise of the sensor changes up and down with the change of the working point of the interferometer. In MI with lengths of the two arms precisely matched, the background noise mainly comes from the circuit noise of electrical devices such as photodetectors and data acquisition card, and the shot noise of photodetectors [13]. The power of circuit noise is relatively constant and small, but the power of the shot noise change with the optical power entering the photodetector, which is the main cause of unstable noise.

The associate editor coordinating the review of this manuscript and approving it for publication was Kin Kee Chow.

The problem of unstable noise can be solved by controlling the working point of the MI. However, the control requires a well-designed feedback algorithm and a piezoelectric transducer (PZT) in the sensing fiber [14], making the MI system more complex and weakening the anti-electromagnetic interference capability of the sensor. To solve the above problems, we propose a new sound extraction algorithm based on the shot noise theory to replace the traditional phase demodulation algorithm based on 3 × 3 couplers. This new algorithm can smooth the unstable noise caused by the change of the working point of the interferometer and does not affect the quality of voice monitoring. This method is completely realized by software, making the MI voice monitoring system more practical.

II. SYSTEM AND THEORETICAL ANALYSIS

A. SYSTEM CONFIGURATION

The voice monitoring system based on Michelson interferometer is shown in Figure 1. A distributed feedback (DFB) laser with a center wavelength of 1550.12 nm and very low intensity noise serves as the light source in this system. An optical isolator (OI, Flyboer Technology) is used to prevent the reflected light from entering the laser. A 2×2 coupler (2 × 2 OC, Flyboer Technology) with a ratio of 1:1 is used to connect the laser part and the interferometer part, leading the backlight from the first arm of the 3 × 3 coupler (3 × 3 OC, Flyboer Technology) to the photodetector 1 (PD1, CPFS934-100, Wuhan Telecommunication Devices). The photodetector 2 (PD2) and the photodetector 3 (PD3) directly detect the backlight of the other two arms of the 3 × 3 coupler, ensuring that the detected three beams have a phase difference of 120° between two [15]. In this structure, the combination of OI and 2 × 2 OC can also be replaced by a fiber circulator. The devices mentioned above are placed in the monitoring room. The signals detected by the photodetectors are input to the monitoring computer (MC, ADLINK Technology) through a data acquisition card (DAQ, PCI-6122, National Instruments) for data processing.

Part (1) and part (2) in Figure 1(a) show the Michelson interferometer and constitute the sound detection probe. Part (1) is the sensing arm loosely fixed on part (2) and exposed to the testing environment to detect sound signals in the environment. Part (2) includes the reference arm and 3 × 3 coupler, which are enclosed in a small plastic box filled with polyurethane foam (PU foam, SKSHU Paint). Polyurethane foam has the properties of sound insulation and heat insulation [16]. Such a package can help to reduce the influence from the reference arm to keep the working point relatively stable and increase the signal-to-noise ratio of the detected signal. The lengths of the sensing arm and the reference arm are both about 20 m with the length difference controlled within 1 cm. Since the length difference is much smaller than the coherent length of the light source, the phase noise caused by the length difference can be ignored [17]. The Faraday Rotating Mirror (FRM, Flyboer Technology) with a pigtail

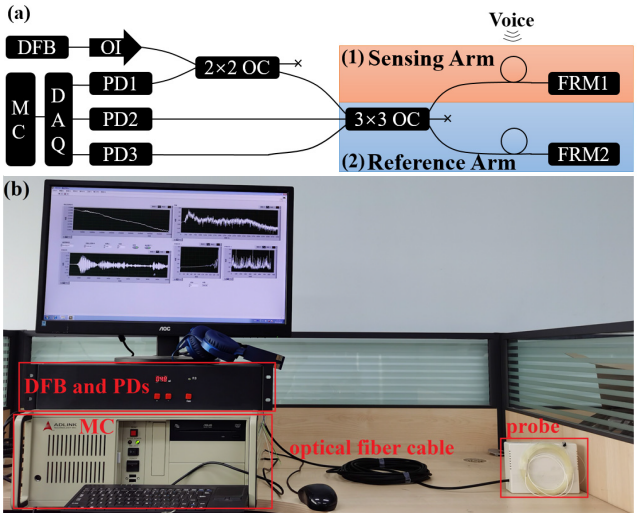

FIGURE 1. Voice monitoring system based on Michelson interferometer. (a) Schematic diagram. (b) A picture of the system.

is spliced to the sensing fiber by fusion and used to avoid polarization fading [18].

As shown in figure 1(b), the DFB light source, three photodetectors and other photoelectric devices are packed in a black box. The sound probe is connected to the black box in the monitoring room through an optical fiber cable, ensuring no active device is put outside the monitoring room when the probe is put outside. Consequently, the anti-electromagnetic interference capability of the system can be guaranteed.

B. ANALYSIS OF DEMODULATION ALGORITHM

According to the interference theory, without considering noise, the signals detected by PDs can be expressed as:

$$I_{PD1} = 2E_{01}^2\{1 + \cos[\Delta\varphi_v(t) + \Delta\varphi_d(t)]\} \quad (1)$$

$$I_{PD2} = 2E_{02}^2\{1 + \cos[\Delta\varphi_v(t) + \Delta\varphi_d(t) + \psi]\} \quad (2)$$

$$I_{PD3} = 2E_{03}^2\{1 + \cos[\Delta\varphi_v(t) + \Delta\varphi_d(t) - \psi]\} \quad (3)$$

where E_{01}, E_{02}, E_{03} are the amplitudes of the sensing light, $\Delta\varphi_v(t)$ is the small phase change caused by the voice in the environment with amplitude less than 1 rad generally, $\Delta\varphi_d(t)$ is the slow phase drift caused by stress relief or temperature change of the sensing fiber. This kind of slow drift causes the change of the working point. The fixed phase difference introduced by the 3 × 3 coupler is $2\pi/3$.

By removing the direct current in the signal and normalizing the amplitude, the three signals can be shown as:

$$I'_{PD1} = \cos[\Delta\varphi_v(t) + \Delta\varphi_d(t)] \quad (4)$$

$$I'_{PD2} = \cos[\Delta\varphi_v(t) + \Delta\varphi_d(t) + \psi] \quad (5)$$

$$I'_{PD3} = \cos[\Delta\varphi_v(t) + \Delta\varphi_d(t) - \psi] \quad (6)$$

In order to compare the traditional phase demodulation algorithm based on 3×3 coupler [19] and the sound extraction algorithm we proposed, the two algorithms will be introduced in the following 1) and 2).

1) ARCTAN METHOD

In this method, all noises are not considered and only two signals are used. Add and subtract I'_{PD2} and I'_{PD3} respectively to get:

$$P_+(t) = I'_{PD2} + I'_{PD3} = -\cos[\Delta\varphi_v(t) + \Delta\varphi_d(t)] \quad (7)$$

$$P_-(t) = I'_{PD2} - I'_{PD3} = \sqrt{3}\sin[\Delta\varphi_v(t) + \Delta\varphi_d(t)] \quad (8)$$

Then the demodulated phase can be expressed as:

$$\Delta\varphi_v(t) + \Delta\varphi_d(t) = -\arctan(\frac{P_-(t)}{P_+(t)})/\sqrt{3} \quad (9)$$

Since $\Delta\varphi_v(t)$ and $\Delta\varphi_d(t)$ consist of high frequency component and low frequency component respectively, $\Delta\varphi_v(t) + \Delta\varphi_d(t)$ can be separated by a high-pass filter to obtain $\Delta\varphi_v(t)$. In the following, we call this algorithm as arctan method.

2) NOISE-STABLE METHOD

In this method, the shot noise of the photodetector and the circuit noise generated by circuits are considered. The shot noise of the photodetector is proportional to the square root of the intensity of the measured light [13], which mainly depends on $\Delta\varphi_d(t)$ at a certain moment t. Therefore, take the first signal I_{PD1} as an example, the shot noise in I_{PD1} is expressed as:

$$n_{sh1}(t)\sqrt{A\cos[\Delta\varphi_d(t)] + D}, \quad D > A \quad (10)$$

where A is the amplification factor of the AC term, and D is the DC component of the signal. A and D depend on the light intensity entering the photodetector, the bias of the photodetector and the amplification factor of circuit. In practice, the specific values of A and D do not need to be measured. We just need to adjust the settings of A and D in the algorithm to obtain the best noise stability. The circuit noise generated by photoelectric detection and data acquisition does not change with measured light [13]. The photodetectors used in our system are integrated on the same circuit board, thus the circuit noise is same for three signals, expressed as $n_e(t)$. Taking the first signal as an example, the signal considering the noise is expressed as I^*_{PD1}.

$$I^*_{PD1} = \cos[\Delta\varphi_v(t) + \Delta\varphi_d(t)] + n_{sh1}(t)\sqrt{A\cos[\Delta\varphi_d(t)] + D} + n_e(t) \quad (11)$$

A zero-phase low-pass filter with a cutoff frequency of 100 Hz is used to separate low frequency and high frequency components in I^*_{PDi} (i = 1, 2, 3). The zero-phase filter can ensure that no phase error is introduced into the final demodulated signal [20]. For I^*_{PD1}, since the low frequency drift of the working point is mainly caused by $\Delta\varphi_d(t)$, $\cos[\Delta\varphi_d(t)]$ can be obtained after zero-phase low-pass filtering. For I^*_{PD2} and I^*_{PD3}, $\cos[\Delta\varphi_d(t) + \psi]$ and $\cos[\Delta\varphi_d(t) - \psi]$ can be obtained respectively. Taking the first signal as an example, the high frequency component in I^*_{PD1} is obtained by subtracting $\cos[\Delta\varphi_d(t)]$ from I^*_{PD1}. Then $\{I^*_{PD1} - \cos[\Delta\varphi_d(t)]\}$ is divided by $\sqrt{A\cos[\Delta\varphi_d(t)] + D}$ to get V_1, expressed as (12).

$$\begin{aligned} V_1 &= \{I^*_{PD1} - \cos[\Delta\varphi_d(t)]\}/\sqrt{A\cos[\Delta\varphi_d(t)] + D} \\ &= \{(\cos[\Delta\varphi_v(t)] - 1)\cos[\Delta\varphi_d(t)] \\ &\quad - \sin[\Delta\varphi_v(t)]\sin[\Delta\varphi_d(t)] \\ &\quad + n_e(t)\}/\sqrt{A\cos[\Delta\varphi_d(t)] + D} + n_{sh1}(t) \end{aligned} \quad (12)$$

Term $(\cos[\Delta\varphi_v(t)] - 1)\cos[\Delta\varphi_d(t)] - \sin[\Delta\varphi_v(t)]\sin[\Delta\varphi_d(t)]$ represents the sensitivity change of the sound sensor with the drift of the working point. We call this term as VS. When $\Delta\varphi_d(t) \approx n\pi + \pi/2$ (n = 0, 1, 2, ...), VS $\approx \pm \sin[\Delta\varphi_v(t)] \approx \pm\Delta\varphi_v(t)$. When $\Delta\varphi_d(t) \approx n\pi$ (n = 0, 1, 2, ...), VS $\approx \pm (\cos[\Delta\varphi_v(t)] - 1) \approx \pm 0.5[\Delta\varphi_v(t)]^2$. Since $\Delta\varphi_v(t) \ll 1$, $|\Delta\varphi_v(t)| \gg 0.5[\Delta\varphi_v(t)]^2$. Thus when $\Delta\varphi_d(t) \approx n\pi + \pi/2$ (n = 0, 1, 2, ...), the sensitivity of sound sensor is higher. At this time, V_1 can be simplified as (13).

$$V_1 \approx [\pm\Delta\varphi_v(t) + n_e(t)]/\sqrt{A\cos[\Delta\varphi_d(t)] + D} + n_{sh1}(t) \quad (13)$$

I^*_{PD2} and I^*_{PD3} are under the same processing as formula (12) to get V_2 and V_3. When $\Delta\varphi_d(t) + 2\pi/3 \approx n\pi + \pi/2$ (n = 0, 1, 2, ...) and $\Delta\varphi_d(t) - 2\pi/3 \approx n\pi + \pi/2$ (n = 0, 1, 2, ...), the second signal and third signal have higher sensitivity respectively.

$$V_2 \approx [\pm\Delta\varphi_v(t) + n_e(t)]/\sqrt{A\cos[\Delta\varphi_d(t) + \psi] + D} + n_{sh2}(t) \quad (14)$$

$$V_3 \approx [\pm\Delta\varphi_v(t) + n_e(t)]/\sqrt{A\cos[\Delta\varphi_d(t) - \psi] + D} + n_{sh3}(t) \quad (15)$$

Since the three signals have a fixed phase difference of $2\pi/3$, the most sensitive one among the three signals can be determined at any time t. The method of selection is to compare the values of $\cos[\Delta\varphi_d(t)]$, $\cos[\Delta\varphi_d(t) + 2\pi/3]$, $\cos[\Delta\varphi_d(t) - 2\pi/3]$. At each moment t, V_i (i = 1, 2, 3) corresponding to the middle value of these three values is used as sound signal. For example, if at a certain t_m, $\cos[\Delta\varphi_d(t_m) + 2\pi/3] > \cos[\Delta\varphi_d(t_m) - 2\pi/3] > \cos[\Delta\varphi_d(t_m)]$, V_3 has the best sensitivity and is selected as sound signal at t_m. This selection can ensure the sensor has the best sensitivity at every time.

After the above mentioned processing, $n_{sh1}(t)$, $n_{sh2}(t)$ and $n_{sh3}(t)$ in V_i (i = 1, 2, 3) do not contain any coefficient related to $\Delta\varphi_d(t)$. Thus the fluctuation of noise intensity caused by the change of the working point is suppressed. When A and D are small, the change in V_i (i = 1, 2, 3) caused by the square root term in V_i (i = 1, 2, 3) is also small, which can be ignored. Thus $\pm\Delta\varphi_v(t)$ without noise fluctuation can be obtained through the above processing. Since sound signal is not sensitive to phase (positive or negative), the final result is expressed as $\Delta\varphi_v(t)$. We call this sound extraction algorithm as noise-stable method, shown in Figure 2.

$\Delta\varphi_v(t)$ obtained by the above two methods can be converted into a sound signal and played in the speaker after down-sampling. Both of these two algorithms can be easily realized for a computer. For each signal frame, the time for

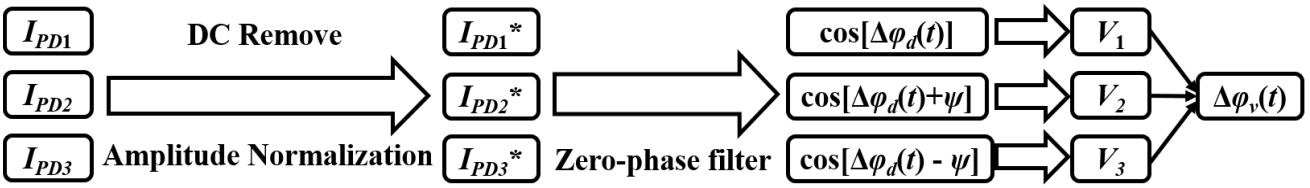

FIGURE 2. Schematic diagram of the noise-stable method.

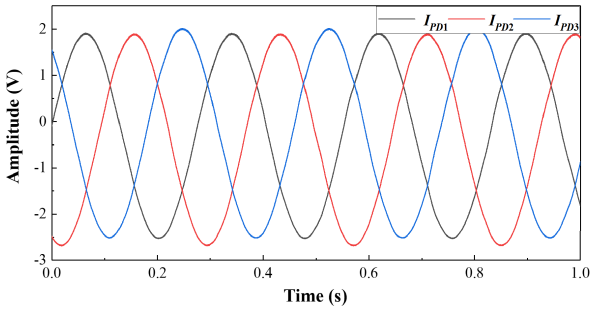

FIGURE 3. Original signals when the sensor is in silent environment.

signal processing is less than the time for sampling. Thus the data acquisition and the signal processing can run continuously and real-time voice monitoring can be realized.

III. EXPERIMENTAL RESULTS AND DISCUSSION

A. EXPERIMENTS IN SILENT ENVIRONMENT

In order to prove the noise-stable method has good stability, we carry out some experiments to compare the noise-stable method with the traditional arctan method. The electrical signals detected by the three photodetectors are converted into digital signals through the data acquisition card PCI-6122 (National Instruments), and the sampling rate is set to 100kS/s. The arctan method and noise-stable method are realized by LabVIEW software. The same original signals are demodulated through these two methods respectively to compare the performance of the two algorithms.

The fiber sensor is placed in a quiet environment in the first part of experiments. After the sensing fiber is disturbed or temperature changes, thermal expansion and contraction with stress relief inside the fiber will cause the change of the length and the refractive index of sensing fiber, resulting in the change of $\Delta\varphi_d(t)$. After a press to the sensor by hand, the original signals detected by the photodetectors are shown in Figure 3. At this time, the working point of the interferometer is in an unstable state.

As the blue plotted curve in Figure 4, the noise intensity of $\Delta\varphi_v(t)$ demodulated by the arctan method fluctuates with the working point shown in Figure 3. When I_{PD2} and I_{PD3} drift to the lower intersection point of about -1.5 V, the corresponding noise intensity reaches the minimum, and when I_{PD2} or I_{PD3} drifts to its maximum value of about 2 V, the corresponding noise intensity reaches the maximum. Due to the ignorance of the shot noise of the photodetectors in arctan

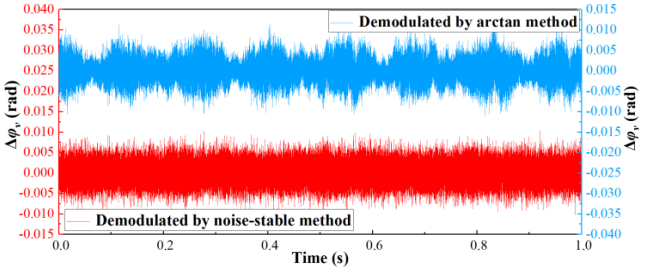

FIGURE 4. $\Delta\varphi_v(t)$ demodulated by arctan and noise-stable method.

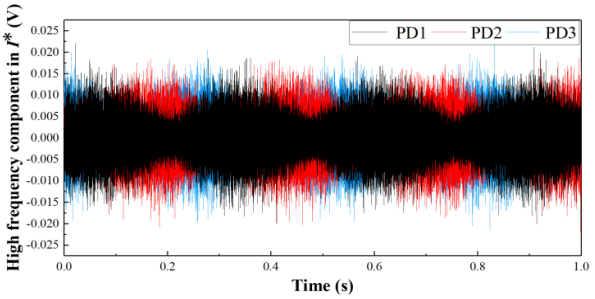

FIGURE 5. High frequency component in I^*_{PD1}, I^*_{PD2} and I^*_{PD3}.

method, such noise fluctuation with the working point occurs. The amplitude of $\Delta\varphi_v(t)$ can reach about 0.008 rad and only 0.003 rad in minimum. After down-sampling, $\Delta\varphi_v(t)$ is converted into sound signal and played out. The unstable noise can be heard.

Figure 5 shows the high frequency component of the original signal after the zero-phase filtering in the noise-stable method, which is the $\{I^*_{PD1} - \cos[\Delta\varphi_d(t)]\}$ in equation (12) (same for the second and third signals). In the silent environment, this component consists of shot noise and circuit noise, thus the maximum value of high frequency noise occurs when the corresponding original signals reach the maximum value.

In the noise-stable method, on the condition of $A = 2$, $D = 3$, the demodulated $\Delta\varphi_v(t)$ with a stable noise intensity is shown in Figure 4 and plotted in red. No fluctuation of noise intensity is observed and the sound played out is stable, matching up with silence in the testing environment.

Two spectrograms can be obtained by implying short time Fourier transform (STFT) to $\Delta\varphi_v(t)$ demodulated by the two algorithms respectively, as shown in Figure 6. Each spectrogram consists of the results of 1000 fast Fourier transforms with Hamming window and the sampling rate of 100kS/s. Spectrograms clearly show the sound power of any frequency

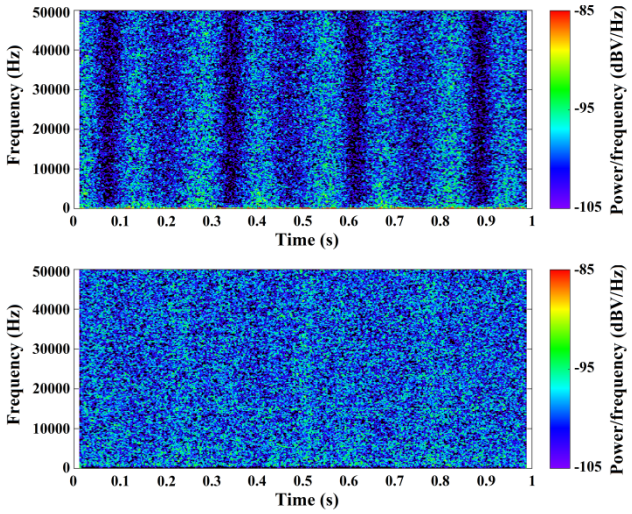

FIGURE 6. Spectrograms of $\Delta\varphi_V(t)$ demodulated by: (a) arctan method, (b) noise-stable method.

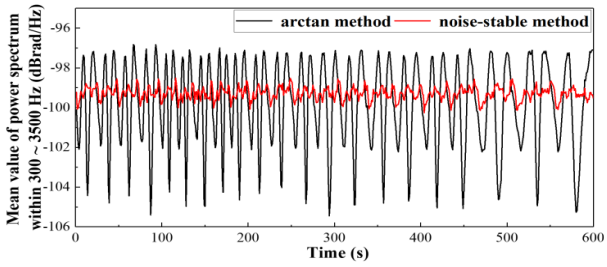

FIGURE 7. Mean value of power spectrum of noise within 300∼3500 Hz.

at any time. In Figure 6(a), some horizontal stripes are visible, meaning that the distribution of noise intensity in the time axis is not uniform and leading to noise intensity fluctuation which can be heard. Relatively the noise distribution shown in Figure 6(b) is uniform, proving that the noise-stable method is effective in suppressing the intensity fluctuation caused by shot noise.

Since the frequency range of human voice is about 300∼3500 Hz and the sensitive range of ear is also concentrated in this frequency band, the sound extracted by above-mentioned methods is always filtered by a band-pass filter to realize voice monitoring in some applications. An experiment is carried on to compare the quality of voice monitoring using arctan method and noise-stable method respectively. The mean value of power spectrum of noise within 300∼3500 Hz is recorded for 10 minutes, meanwhile the working point of interferometer slowly drifts with a frequency under 1 Hz. The test results are shown in Figure 7. For arctan method, the fluctuation range of this mean value is within −95∼−105 dB, leading to significant intensity change. For noise-stable method, the fluctuation range does not exceed 2 dB, meaning that it has good stability.

According to the experimental results, the main difference between the two algorithms is that they have different sound effects in a silent environment. The root cause of this difference is there are two different distributions in the original

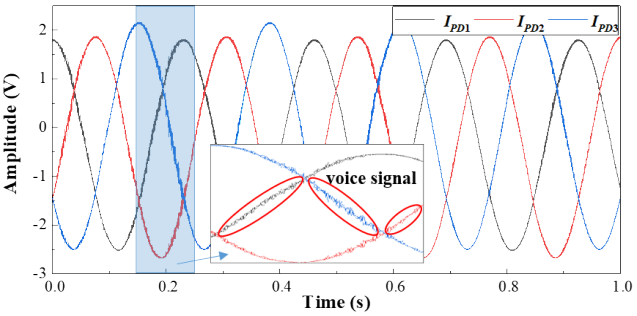

FIGURE 8. Original signals detected by the photodetectors with voice.

signal. For the shot noise, noise intensity increase with the voltage of original signals, which is shown in Figure 5 and corresponding Figure 3. While for the sound signal, the high sensitivity states occur when the voltage of original signals are at a middle level, which is determined by interference formulas (1), (2) and (3). The two different distributions coexist in the same original signals.

The traditional arctan method only deals with the distribution of the sound signal. If the arctan method is used, when the shot noise cannot be ignored, the demodulated sound signal will be affected by fluctuations of the shot noise. As shown in Figure 6 and Figure 7, the shot noise affects the whole frequency band, including 300∼3500 Hz, which brings bad effects to the quality of sound monitoring. Therefore, we propose the noise-stable method, which is designed to demodulate sound signals from original signals and give consideration to the distribution of shot noise at the same time. Thus using the noise-stable method, the background noise of sound monitoring is more stable.

B. EXPERIMENTS WITH VOICE

In this part, the ability of noise-stable method to demodulate voice signal is tested. A cellphone is used as a voice source to play an audiobook by its speaker. The optical fiber sensor is placed nearby the cellphone to detect the voice signal.

Figure 8 shows the original signals detected by the photodetectors when there is voice in the environment. By zooming in the displayed original signals, some weak voice signals can be seen.

The V_1, V_2 and V_3 obtained by the noise-stable method are shown in Figure 9, each of them contains the voice signal to be tested, but cannot continuously achieve high sensitivity voice detection alone due to the sensitivity change with the working point. However, at any time t, one of the three signals is always in a state of high sensitivity. For example, the signals in the red circle in Figure 8 are in a state of high sensitivity. The segments with high sensitivity in each signal are taken out by the judgment of middle value of $\cos[\Delta\varphi_d(t)]$, $\cos[\Delta\varphi_d(t)+2\pi/3]$, $\cos[\Delta\varphi_d(t)-2\pi/3]$ and spliced together.

After down-sampling, the sound signal containing voice to be tested is obtained, as shown in Figure 10.

Comparing Figure 9 with Figure 10, it can be found that the sound signal in Figure 10 is mainly composed of the

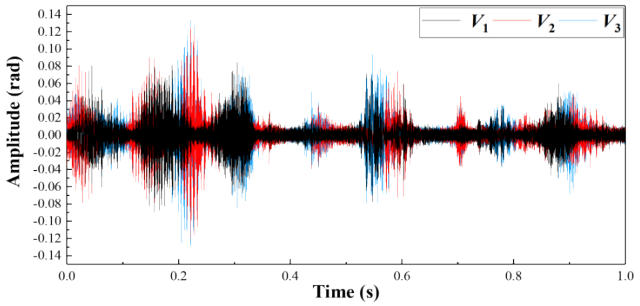

FIGURE 9. V_1, V_2 and V_3 obtained by the noise-stable method.

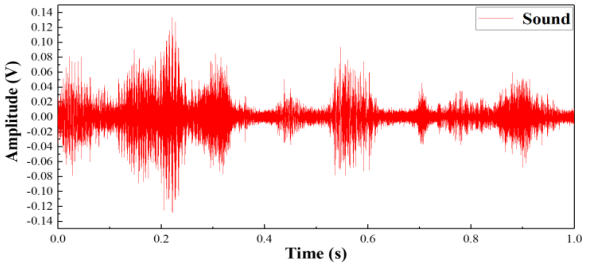

FIGURE 10. Voice extracted by noise-stable method.

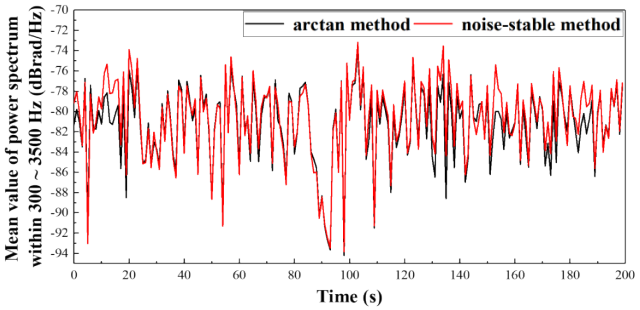

FIGURE 11. Mean value of power spectrum of voice within 300∼3500 Hz.

maximum values of each signal in Figure 9. Duo to the voice demodulated by the noise-stable method uses the most sensitive parts of V_1, V_2 and V_3, the monitored voice has good quality and stability.

In an environment with voice, the mean value of power spectrum of $\Delta\varphi_v(t)$ within 300∼3500 Hz is recorded for 200 seconds, as shown in Figure 11. For the sound signals demodulated by the two methods, the change of this mean value is basically the same, proving that the signal processing using the noise-stable method does not adversely affect the voice quality.

IV. CONCLUSION

In conclusion, a Michelson optical fiber voice monitoring system is introduced and a novel sound extraction algorithm is proposed. The algorithm called noise-stable method can demodulate voice signal with high stability of noise intensity and high sensitivity to realize stable voice monitoring. The fluctuation range of noise intensity in 300∼3500 Hz decrease from 10 dB to less than 2 dB compared with the traditional phase demodulation algorithm. Such a method and a system have broad application potential in voice monitoring.

CONFLICT OF INTERESTS

The authors declare no conflict of interest.

ACKNOWLEDGMENT

The authors would like to thank Hongyan Wu and Huang Tang from Fudan University for their valuable discussions on article writing.

REFERENCES

[1] C. K. Kirkendall and A. Dandridge, "Overview of high performance fibre-optic sensing," *J. Phys. D, Appl. Phys.*, vol. 37, no. 18, pp. 197–216, 2004.

[2] Y. Wang, H. Yuan, X. Liu, Q. Bai, H. Zhang, Y. Gao, and B. Jin, "A comprehensive study of optical fiber acoustic sensing," *IEEE Access*, vol. 7, pp. 85821–85837, 2019.

[3] Z. Ye, J. Wang, C. Wang, and B. Jia, "A positioning algorithm realized multilateration for distributed fiber-optic sensor," *Microw. Opt. Technol. Lett.*, vol. 58, no. 12, pp. 2913–2917, Dec. 2016.

[4] E. Udd, "Fiber-optic acoustic sensor based on the Sagnac interferomete," *Proc. SPIE*, vol. 0425, pp. 90–95, Nov. 1983.

[5] S. Qian, H. Chen, Y. Xu, L. Zhong, and L. Su, "A distributed fiber sensing system for acoustic emission and vibration of power equipment," in *Proc. Int. Conf. Condition Monitor. Diagnosis (CMD)*, Sep. 2016, pp. 802–805.

[6] P. Gartland, "Fiber-optic michelson interferometer with Faraday mirrors for acoustic sensing using a 3 × 3 coupler and symmetric demodulation scheme," M.S. thesis, Dept. Electron. Eng., Virginia Tech, Blacksburg, VA, USA, 2016.

[7] S. Liang, C. Zhang, W. Lin, L. Li, C. Li, X. Feng, and B. Lin, "Fiber-optic intrinsic distributed acoustic emission sensor for large structure health monitoring," *Opt. Lett.*, vol. 34, no. 12, pp. 1858–1860, Jun. 2009.

[8] J. Liu, L. Yuan, J. Huang, and H. Xiao, "A cantilever based optical fiber acoustic sensor fabricated by femtosecond laser micromachining," *Proc. SPIE*, vol. 9738, Apr. 2016, Art. no. 973804.

[9] H. Tsuda, E. Sato, T. Nakajima, H. Nakamura, T. Arakawa, H. Shiono, M. Minato, H. Kurabayashi, and A. Sato, "Acoustic emission measurement using a strain-insensitive fiber Bragg grating sensor under varying load conditions," *Opt. Lett.*, vol. 34, no. 19, pp. 2942–2944, 2009.

[10] Z. Wang, B. Zhang, J. Xiong, Y. Fu, S. Lin, J. Jiang, Y. Chen, Y. Wu, Q. Meng, and Y. Rao, "Distributed acoustic sensing based on pulse-coding phase-sensitive OTDR," *IEEE Internet Things J.*, vol. 6, no. 4, pp. 6117–6124, Aug. 2019.

[11] T. Zhu, Q. He, X. Xiao, and X. Bao, "Modulated pulses based distributed vibration sensing with high frequency response and spatial resolution," *Opt. Exp.*, vol. 21, no. 3, pp. 2953–2963, Feb. 2013.

[12] C. Wang, C. Wang, Y. Shang, X. Liu, and G. Peng, "Distributed acoustic mapping based on interferometry of phase optical time-domain reflectometry," *Opt. Commun.*, vol. 346, pp. 172–177, Jul. 2015.

[13] H. Zhang, M. Zhang, L. Wang, Y. Liao, and D. N. Wang, "Output noise analysis of optical fiber interferometric sensors using a 3 *times* 3 coupler," *Meas. Sci. Technol.*, vol. 22, no. 12, pp. 125203–125211, 2011.

[14] D. A. Jackson, R. Priest, A. Dandridge, and A. B. Tveten, "Elimination of drift in a single-mode optical fiber interferometer using a piezoelectrically stretched coiled fiber," *Appl. Opt.*, vol. 19, no. 17, pp. 2926–2929, 1980.

[15] B. Chiu and M. C. Hastings, "Digital demodulation for passive homodyne optical fiber interferometry based on a 3 × 3 coupler," *Proc. SPIE*, vol. 2292, pp. 371–382, Nov. 1994.

[16] J. O. Akindoyo, M. D. H. Beg, S. Ghazali, M. R. Islam, N. Jeyaratnam, and A. R. Yuvaraj, "Polyurethane types, synthesis and applications—A review," *RSC Adv.*, vol. 6, no. 115, pp. 114453–114482, 2016.

[17] D. Xu, F. Yang, D. Chen, F. Wei, H. Cai, Z. Fang, and R. Qu, "Laser phase and frequency noise measurement by Michelson interferometer composed of a 3 × 3 optical fiber coupler," *Opt. Exp.*, vol. 23, no. 17, pp. 22386–22393, 2015.

[18] S.-T. Shih, M.-H. Chen, and W.-W. Lin, "Analysis of fibre optic michelson interferometric sensor distortion caused by the imperfect properties of its 3 × 3 coupler," *IEE Proc. Optoelectron.*, vol. 144, no. 6, pp. 377–382, Dec. 1997.

[19] H. Wu, Y. Feng, H. Xu, and D. Zhao, "A new demodulation method to improve the sensitivity and dynamic range of fiber optic interferometric system," in *Proc. 9th Int. Conf. Opt. Commun. Netw. (ICOCN)*, Oct. 2010, pp. 70–72.
[20] Y. Xiao, M. Zhang, and K. Wang, "The implementation of zero-phase, high-pass filtering in interferometric fiber-optic hydrophone system," *Proc. SPIE*, vol. 8561, Nov. 2012, Art. no. 85611J.

YUHAN HU received the B.S. degree from Fudan University, Shanghai, China, in 2018, where he is currently pursuing the Ph.D. degree with the Fiber-Optic Research Center, Department of Materials Science. His research interests include optical fiber sensors and signal processing.

QIUHENG SONG received the B.S. degree from the University of Electronic Science and Technology of China, Chengdu, China, in 2014, and the M.S. and Ph.D. degrees from Fudan University, Shanghai, China, in 2017 and 2020, respectively. He is currently a Postdoctoral Fellow with Fudan University. His research interests include optical fiber sensors and signal processing.

HEKUO PENG received the B.S. and Ph.D. degrees from Fudan University, Shanghai, China, in 2013 and 2018, respectively. He is currently a Postdoctoral Fellow with Fudan University. His research interests include optical fiber sensors and pattern recognition.

QIAN XIAO received the B.S. degree from Beihang University, Beijing, China, in 1995, and the Ph.D. degree from Fudan University, Shanghai, China, in 2013. She is currently an Assistant Professor in physical electronics with Fudan University. Her research interests include optical fiber sensors and optical fiber communication.